Desalination and Water Treatment
www.deswater.com
doi: 10.1080/19443994.2015.1072057

57 (2016) 15373–15383
July

Taylor & Francis
Taylor & Francis Group

Citric acid modified *Camellia oleifera* shell for removal of crystal violet and Pb(II): parameters study and kinetic and thermodynamic profile

Huiqin Guo, Liushui Yan*, Dongyang Song, Kexin Li

Key Laboratory of Jiangxi Province for Persistent Pollutants Control and Resources Recycle, School of Environmental and Chemical Engineering, Nanchang Hangkong University, Nanchang 330063, P.R. China, email: huiqinguo2013@gmail.com (H.Q. Guo), Tel. +86 791 3953787; Fax: +86 791 3953373; emails: yanliushui@nchu.edu.cn (L.S. Yan), 786813055@qq.com (D.Y. Song), likx880@hotmail.com (K.X. Li)

Received 6 December 2014; Accepted 4 July 2015

ABSTRACT

Chemically modified *Camellia oleifera* shell (CA-COS) was prepared by means of solid-phase esterifying technique. The adsorption of crystal violet (CV) and Pb(II) onto CA-COS were studied and the effect of various parameters such as solution pH, ion strength, and the initial concentration of contaminant on the adsorption were investigated. The adsorption kinetics, adsorption isotherms, and thermodynamic behaviors were also studied. The pseudo-first-order, pseudo-second-order, and intraparticle diffusion models were employed to describe the kinetic behaviors of the adsorption in different initial contamination concentrations, and it was found that the adsorption processes followed the pseudo-second-order model very well. The adsorption equilibrium data fitted to the Langmuir isotherm (R^2 = 0.9996 and 0.9992 for CV and Pb(II), respectively) well, and the adsorption capacity of CA-COS to CV and Pb(II) were 120.5 and 45.2 mg g^{-1}, respectively. The thermodynamic results indicated the adsorption of CV and Pb(II) on CA-COS is endothermic and can proceed spontaneously.

Keywords: Citric acid modified *Camellia oleifera* shell (CA-COS); Adsorption; Crystal violet; Lead ions; Wastewater treatment

1. Introduction

Heavy metals and synthetic dyestuffs are the main pollution components of the industrial effluent, which come from various industries such as textiles, pigments, papers, plastics, mining, and metallurgical processes. Because of the ecotoxicological effects, bioaccumulation and cancerogenic effect of these pollutants themselves or the degradation products of dyes on the environment and human being, the wastewater must be treated properly before they were discharged into the environment. Various approaches for their removal have been carried out, such as coagulation, oxidation [1], chemical precipitation, ion exchange, reverse osmosis, phytoextraction, ultrafiltration, membrane separation [2,3], and adsorption. Among those techniques, adsorption offers the simplest and lowest cost method for eliminating the dyestuff or heavy metals from industrial wastewaters, especially before discharging them into water reservoir or environment even if reuse in processing. Although various of materials synthesized (activated

---

*Corresponding author.

carbon, nanocarbon materials such as activated carbon fiber and carbon nanotubes) or natural (zeolite, coal fly ash, agricultural byproducts) origin have been employed or studied for color or heavy metal ions removal from wastewater, considering of the adsorption efficiency, biomasses from forestry and agricultural product which are rich in lignin, cellulose, and hemicellulose are considered to be very beneficial to heavy metals or organic contaminant adsorption, and which has increased great interest of researchers and engineers in wastewater treatment. Besides, because the secondary waste will be minimized and resultant of waste reutilization through this usage, a large number of biomass materials such as kenaf core fibers [4], palm kernel fiber [5], wheat straw [6], maize cob [7], grapefruit peel [8], rice husk [9], coniferous pinus bark [10], sugarcane bagasse [11], and chestnut shell [12] have been widely studied in the heavy metal or dyestuff removal in aqueous solutions.

Camellia oleifera is a branch camellia plant of theaceae, which is the unique and largest woody oil-bearing crop in southern China. *C. oleifera* shell (COS) is the outer coat of the fruit, whose amount accounted for ~60% quality of the whole fruit, which is one of the main byproduct in the tea camellia processing industry. In addition to be used as fuel, large amounts of redundant COS were discharged into environment untreated, resultant of huge bioresource loss and environmental pollution. Previous studies showed that COS composed mainly of the lignin, cellulose, hemicellulose, and tannins (polyphenols) [13], which will be great potential as adsorbent in the field of wastewater treatment. Our previous study has also found that COS can be used in the adsorption removal of crystal violet (CV) from aqueous solution, and to an initial concentration of 50 ppm of CV, the removal rate can reach 98% in the optimum conditions [14]. However, compared to other reported work, the adsorption capacity of untreated COS is not very high (only has ~27 mg g^{-1}), which is lower than that of palm kernel fiber [5], *ananas comosus* (pineapple) leaf powder [15] and coniferous pinus bark powder [10] on contaminants. Chemical modification has usually shown considerable promise in improving the surface property of agricultural byproducts, compared with the untreated biosorbents, the modified ones have reported to increase the adsorption capacity greatly [16–20]. As a flavor and stabilizer, citric acid (CA) is a low-cost chemical, which used extensively in the food industry. After modifying the raw biosorbents with CA, the introduced free carboxyl groups can increase the negative charge on their surface, thereby enhancing which binding capacity for cationic contaminants obviously [4,21,22].

The aim of this study was to prepare a high-efficient COS biosorbent through chemically treating the raw COS with CA by solid-phase esterifying technique, and then applied in the removal of cationic pollutants in aqueous solutions. CV and Pb(II) were selected as the target adsorption species because they are the typical contaminant representatives of cationic dyes and heavy metal ions, respectively. CV is one of the basic dyes, which has been shown to have very harmful effect on living organisms even if on short period of exposure, and Pb(II) can bring substantial threat to human health through the food chains, even though at low concentration [3]. The effect of initial solution pH, ionic strength, and initial contaminant concentration, on adsorption removal of CV and Pb(II) by CA-COS have been investigated; the adsorption kinetics, the adsorption isotherms, and thermodynamics were also studied.

2. Experimental

2.1. Chemicals

1.0 g L^{-1} CV (A.R. Shanghai Fine Chemical Technology Co., Ltd) and Pb(II) ($Pb(NO_3)_2$, A.R., Xilong Chemical Co., Ltd) stock solutions were prepared by dissolving required amount of CV and lead nitrate in deionized water, respectively. CA was purchased from the Shanghai experimental Reagent Co., Ltd, 0.5 mol L^{-1} CA solution was prepared by dissolving certain amount of CA in deionized water, and stored at 4℃ for use. All the other reagents were got from Guangdong Xilong Chemical Co., Ltd. All chemicals and reagents used were analytical reagent grade or above, deionized water was used throughout.

2.2. Preparation and characterization of modified COS

COS used in this study was obtained from Jiangxi Green Sea Oil Co., Ltd. The raw COS was rinsed with water for several times, dried in air, and baked in vacuum oven at 40℃ to a constant weight, then sieved (0.147 mm) and stored in desiccator for use.

The chemical modification of COS was carried out as the method reported [23]. An amount of COS powder was mixed with 0.5 M CA solution at a ratio of 1:12 (w/V, g mL^{-1}), stirred at 500 rpm for 30 min at room temperature, and then dried at 50℃ for 24 h. The thermochemical reaction between CA and COS was proceeded by increasing the oven temperature from room temperature to 120℃ during 90 min, then cooled to room temperature after the reaction finished. The products were transferred and washed with deionized water and filtrated, until no citrate was

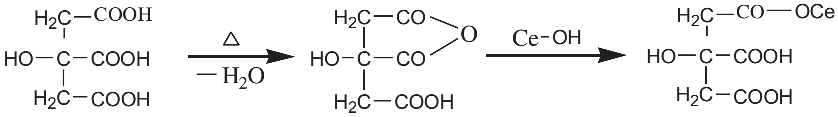

Fig. 1. Reaction of chemical modification of COS by CA.

detected in the liquid. The obtained CA modified COS (CA-COS) was dried at 50°C for 12 h and stored in desiccator for use. The proximate composition of the COS and CA-COS was investigated by FT-IR spectrophotometer (BRUKER VERTEX 70). IR absorbance data were obtained for wavenumbers in the range of 4,000–400 cm^{-1} and analyzed.

The chemical modification of COS can be schematically expressed as Fig. 1.

where C_e represents the cellulose in COS.

2.3. Adsorption experiments

The batch adsorption experiments were conducted for each component. Generally, 0.2 or 0.4 g of CA-COS was added into 100 mL of known concentration of CV or Pb(II) solution in a 250-mL conical flask, respectively; adjusted the pH to the desire, then the solutions were shaken in an oscillator at desired temperature for required time. After the equilibrium was reached, 5 mL of suspension was obtained and centrifuged at 8,000 r min^{-1} for 10 min, and the final contaminant concentration (C_e) in the solution was measured by spectrophotometry at $\lambda = 582$ nm for CV and by atomic absorption spectrometry (AAS) for Pb (II), respectively. All the experiments were carried out in duplicate and the average was used. The equilibrium adsorption capacity (q_e, mg g^{-1}) and the removal percentage (R, %) of CV or Pb(II) from the solutions was calculated with the following equations:

$$q_e = \frac{(C_0 - C_e) \times V}{m} \tag{1}$$

$$R = \frac{C_0 - C_e}{C_0} \times 100\% \tag{2}$$

where q_e is the equilibrium adsorption capacity, mg g^{-1}; C_e is the equilibrium concentration of sorbate, mg L^{-1}; C_e is the initial concentration of sorbate, mg L^{-1}; V is the volume of sorbate solution, L; and m is the dose of adsorbent, g.

The adsorption kinetics experiments were performed by mixing 0.2 or 0.4 g of CA-COS with certain concentration of CV or Pb(II) solutions in 250-mL conical flask, then adjusting pH to 7.0 and 5.0 for the solutions, respectively. The mixtures were oscillated at 20°C and sampled at different time intervals, centrifuged at 8,000 r min^{-1} for 10 min and then volumes of supernatant were taken for analysis. Three different initial concentrations for each contamination were conducted to study the adsorption kinetics. The adsorption dynamic curves of CV and Pb(II) were obtained by the plots of q_t(the adsorption amount at time t, mg g^{-1}) vs. t (min).

The adsorption equilibrium studies were carried out by agitating a series of 250-mL conical flasks containing 0.2 or 0.4 g of CA-COS and 50 mL of CV or Pb(II) solutions with different initial concentrations (50–300 mg L^{-1} CV, or 100–400 mg L^{-1} Pb(II)) in a thermostat rotary shaker at 20, 30, and 40°C, respectively. The adsorption was proceeded for 5 h for CV and 30 min for Pb(II), then sampled and analyzed for CV and Pb(II), respectively, as described above.

3. Results and discussion

3.1. Fourier transform infrared spectroscopy

The surface functional groups presented in the adsorbent could be analyzed by the FT-IR, and the possible adsorption enhancement mechanism after modification could also be verified by comparison of the FT-IR spectrum of COS before and after functionalization. As shown in Fig. 2, for the COS (A), the broad peak near 3,405 cm^{-1} indicated the presence of large numbers of hydroxyl groups in the surface of the COS; the peak observed at 1,739 cm^{-1} could be assigned to the characteristic stretching vibration of C=O band in carboxyl group; the peak 1,043 cm^{-1} was mainly produced by the bending vibration of O–H and the stretching vibration of C–O–C. After the functionalization, two major changes were observed (Fig. 2(B)): (1) the absorption intensity of C=O at 1,739 cm^{-1} was enhanced obviously, and (2) the broad absorption peak of hydroxyl group shifted from 3,405 to 3,448 cm^{-1}, which suggested that carboxylic group was successfully introduced into the surface of the COS after the CA modification. It will be very beneficial to the CV or Pb(II) adsorption in the surfaces.

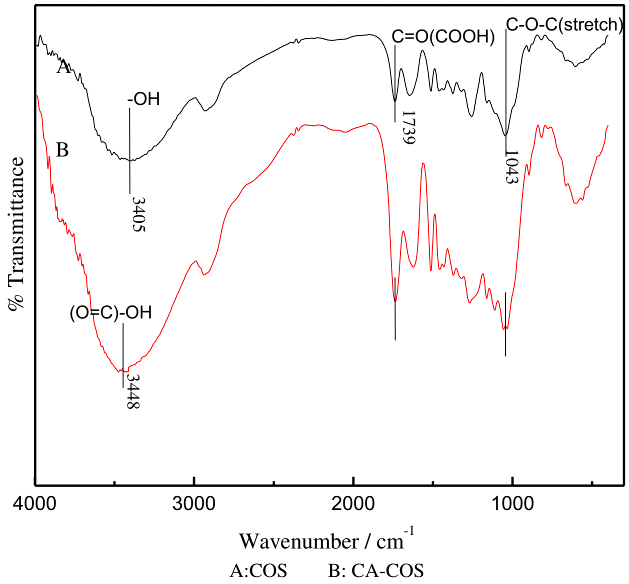

Fig. 2. FT-IR spectra of COS and CA-COS.

3.2. Effect of initial solution pH

The pH value of the contaminant solution is an important factor in the process, which always affects the adsorption through changing the surface properties of the sorbent material and the degree of sorbate ionization [24]. The effect of initial pH on the contaminants adsorption removal was investigated at 20℃, and the pH was adjusted to the tested range by addition of diluted HCl or NaOH solutions. Fig. 3 shows the effect of pH on the removal percent of CV (pH 3.0–9.0) and Pb(II) (pH 3.0–6.0) from solutions. It can be seen from the figure that the *R*% increased from 82.11 to –97% when the pH increased from 3.0 to 7.0, and then kept almost stable to continue increasing the pH to 9.0. For Pb(II), an increase from 72.46 to 86.90% was observed when the pH increased from 3.0 to 4.0, then the removal rate kept almost stable when the pH increased to 5.5, and finally decreased when pH > 5.5.

Based on the above analysis, it can be noticed that it showed lower removal rate of both CV ad Pb(II) at lower pH, which may contribute to that the excess H^+ ions in the high acidic solution competed with the sorbate cations for the adsorption sites. At higher pH value, the surface of the sorbents may be mostly negatively charged, which is very beneficial to the dye cations adsorption. As to heavy metal, its speciation may change due to the secondary hydrolysis process, resultant of decreased removal rate. Very similar results have been reported for the adsorption of CV, methylene blue, Pb(II), Co(II) and Cd(II) on other modified or raw biosorbent [6,25]. Thereby, the pH 7.0 and 5.0 were selected for the following adsorption tests of CV and Pb(II), respectively.

3.3. The effect of NaCl concentration

The effect of the ionic strength on the adsorption of CV and Pb(II) was investigated using NaCl as the interfering salt. As can be seen from Fig. 4, when NaCl concentration increased from 0 to 0.2 mol L^{-1}, the removal rate of CV had no obvious change, i.e. only decreased from 98.2 to 95.6%, but for Pb(II), it

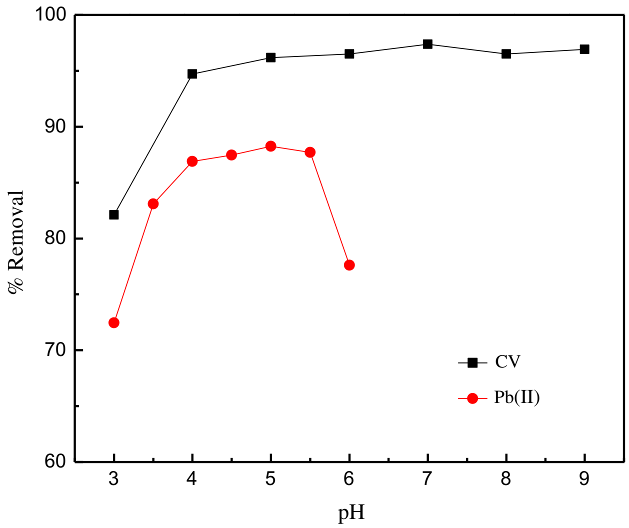

Fig. 3. Effect of solution pH on the adsorption removal of CV and Pb(II) on CA-COS.

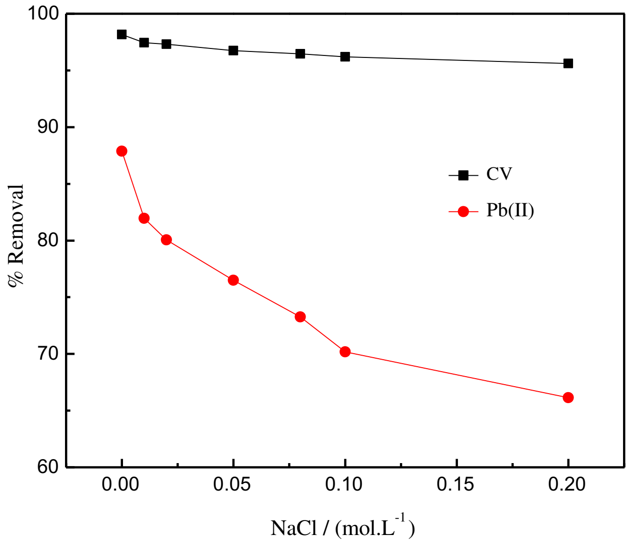

Fig. 4. Effect of NaCl concentration on the adsorption removal of CV and Pb(II) on CA-COS.

declined from 87.9 to 66.1%. Low ionic strength appeared to have negligible impact in the removal of CV by CA-COS, but had significant effect on that of Pb(II).

3.4. Effect of contact time and the adsorption kinetics

Fig. 5 shows the effect of contact time on the adsorption capacity for different initial concentrations of CV (50, 100, and 150 mg L^{-1}) and Pb(II) (80, 100, and 150 mg L^{-1}). As can be seen from Fig. 5(a), for low concentration of CV (50 mg L^{-1}), the adsorption rate was very high and could reach equilibrium only within 30 min. It may due to that at low contaminant concentration, enough active sorption sites existed in the sorbent surface, which is very beneficial for contaminant adsorption. When there was higher concentration of CV, it needed much longer time of 120 and 240 min to get equilibrium with the initial CV concentration of 100 and 150 mg L^{-1}, respectively. As for Pb(II), however, it always showed very rapid sorption in all the tested concentrations, and the equilibrium was attained in ~20 min (Fig. 5(b)). Compared the results of above, it may imply that big molecule (CV) adsorption was affected more by the driving force of concentration gradient than that of small molecule, and the agglomeration of dye stuff molecule in high concentrations may also slow down the adsorption process [26]. As could also be seen from Fig. 5, the adsorption capacity of CV and Pb(II) apparently increased with the increase in the sorbate concentration, which increased from 24.63 to 73.45 mg g^{-1} and from 18.32 to 30.56 mg g^{-1}, with an increase in CV and Pb(II) concentration from 50 to 150 mg L^{-1} and 80 to 150 mg L^{-1}, respectively.

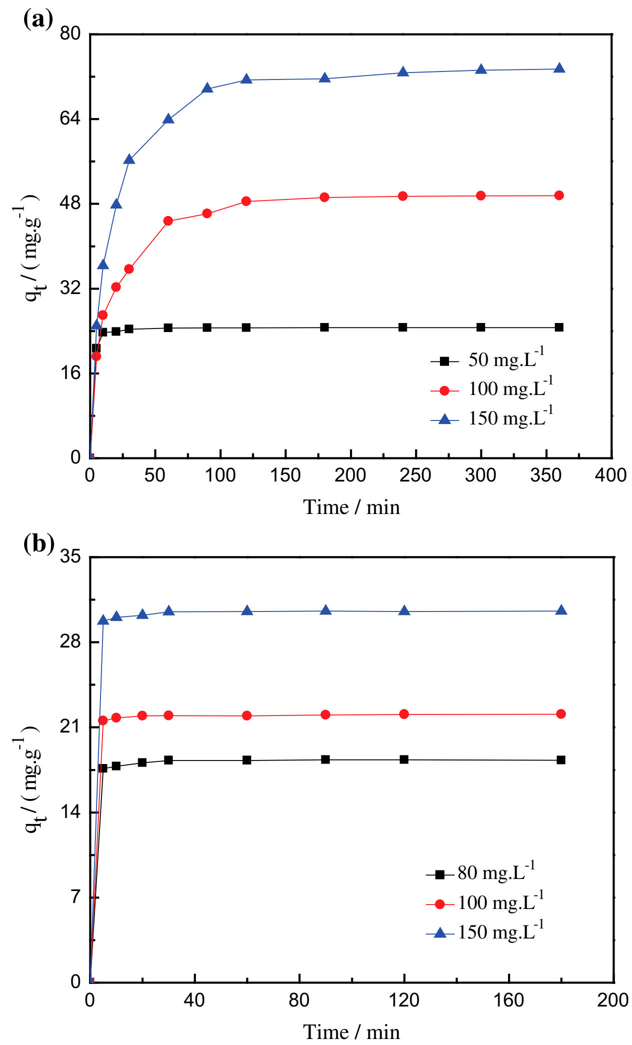

Fig. 5. Effect of contact time on the adsorption of CV and Pb(II) on CA-COS.

In order to examine the controlling mechanism of the sorption process, two kinetics models were used to describe the above adsorption data. The pseudo-first-order model considers the rate of occupation of sorption sites to be proportional to the number of unoccupied sites [8], its linear form can be defined as the following equation:

$$\log(q_e - q_t) = \log q_e - \frac{k_1 \times t}{2.303} \tag{3}$$

where q_e is the equilibrium adsorption capacity, mg g^{-1}; q_t is the adsorption capacity after adsorption time t, mg g^{-1}; k_1 is the first-order reaction rate constant, min^{-1}. The value of q_e and k_1 can be computed from the intercept and slope of a plot of log $(q_e - q_t)$ against t.

The linear form of the pseudo-second-order model was expressed in the following equation:

$$\frac{t}{q_t} = \frac{1}{k_2 q_e^2} + \frac{t}{q_e} \tag{4}$$

where q_t is the adsorption amount of contaminant at any given time t, mg g^{-1}; q_e is the uptake amount of contaminant at equilibrium, mg g^{-1}; k_2 is the second-order reaction rate constant, g mg^{-1} min^{-1}. In addition, the initial adsorption rate h (mg g^{-1} min^{-1}) is defined as $k_2 q_e^2$, which was the rate when $t \rightarrow 0$. The values of q_e, k_2, and h can be calculated from the slope and intercept of the linear plot of t/q_t against t

The above pseudo-first-order and pseudo-second-order models were used to fit the experimental data of CV and Pb(II) adsorption, and the related statistic parameters were presented in Table 1. As can be seen,

Table 1
Adsorption kinetic parameters of CV and Pb(II) on CA-COS

Sorbate	C_0 (mg L^{-1})	The pseudo-first-order model			The pseudo-second-order model				Intraparticle diffusion model	
		$q_{e,cal}$ (mg g^{-1})	k_1 (min^{-1})	R^2	$q_{e,exp}$ (mg g^{-1})	$q_{e,cal}$ (mg g^{-1})	k_2 (L mg^{-1} min^{-1})	R^2	k_{id} (mg g^{-1} min$^{-0.5}$)	R^2
CV	50	0.557	0.0130	0.7003	24.634	24.679	0.0821	1.0000	0.9669	0.6933
	100	22.309	0.0204	0.9843	49.530	51.125	0.0021	0.9997	2.7930	0.9523
	150	41.879	0.0211	0.9258	73.445	75.700	0.0013	0.9999	2.8668	0.9736
Pb(II)	80	0.387	0.0110	0.5648	18.322	18.328	0.2871	1.0000	0.2063	0.9974
	100	0.356	0.0177	0.9124	22.085	22.095	0.2251	1.0000	0.1321	0.9052
	150	0.390	0.0157	0.6512	30.558	30.581	0.2156	1.0000	0.2168	0.9750

Note: $q_{e,cal}$ is the calculative equilibrium adsorption capacity; $q_{e,exp}$ is the experimental equilibrium adsorption capacity.

in all CV and Pb(II) concentrations tested, high correlation coefficients ($R^2 > 0.9997$) were obtained in the case of pseudo-second-order kinetics, and the calculated $q_e$values agreed well with the experimental data. It suggests that the rate-limiting step of CV and Pb(II) adsorption on CA-COS may be chemisorption process, i.e. the chemical interactions possibly occur between superficial functional groups of biosorbent with the heavy metal ions or dyes. Similar behavior has been reported for other types of biosorbent [25]. It also can be seen from Table 1 that the initial adsorption rate (h) of Pb(II) increased from 96.44 to 201.63 mg g^{-1} min^{-1} with the initial concentration increased from 50 to 150 mg L^{-1}; but the h value for CV was very high in the tested low concentration, and very low in higher concentration. It suggested that the concentration gradient may be the primary driving force for metal ions adsorption in the CA-COS surface in the very initial of the process. As to CV, however, higher concentration would result in the clustering of the molecule due to the effect of hydrogen bond and Van der Waals' force in their hydrophobic part, which but not the adsorption in the biosorbents plays the main role in the process [26].

Lagergren pseudo-first-order and pseudo-second-order rate models cannot identify the diffusion mechanism during the sorption process and uptake varies almost proportionately with the half-power of time, $t^{0.5}$, rather than t. The intraparticle diffusion model was considered to determine the participation mechanism of the sorption of CV and lead ion in CA-COS. The diffusion model is expressed by the following equation:

$$q_t = k_{id} t^{0.5} + C \tag{5}$$

where q_t is the adsorption capacity after adsorption time , mg g^{-1}; k_{id} is the intraparticle diffusion rate constant, mg g^{-1} min$^{-0.5}$; C is a constant. If the regression is linear and passes through the origin, then intraparticle diffusion is the rate-limiting step; if the plot of q_e vs. $t^{0.5}$ is linear but does not pass through the origin, suggesting that adsorption involve intraparticle diffusion. The plots and the calculated parameters were shown in Fig. 6 and Table 1, respectively. It can be seen that the adsorption process for CV and Pb(II) has significant difference in the plots. It was divided into three stages for CV adsorption, i.e. the first sharper portion being a rapid external surface adsorption which was contributed to the large surface area of the adsorbents, and always was available at the beginning of the adsorption process; the second linear portion

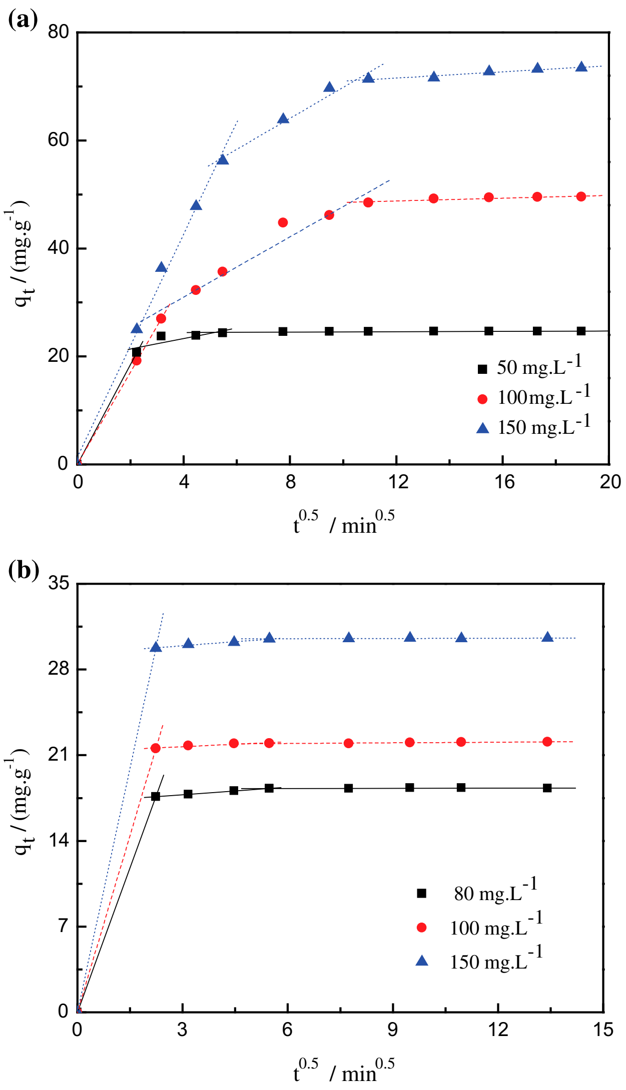

Fig. 6. Intraparticle diffusion models for the adsorption of (a) CV and (b) Pb(II) on CA-COS.

being a gradual adsorption which was the rate-limiting step, and the final portion being an equilibrium stage (Fig. 6(a)). It can be seen from the values of intraparticle diffusion rate constant in second phase (k_{idII}) that with the initial CV concentration increased from 50 to 150 mg L^{-1}, k_{id}II was enhanced from 0.1872 to 3.6551 mg g^{-1} $min^{-0.5}$. However, the metal ion adsorption can reach equilibrium in a very short time, so this process does not fit the intraparticle diffusion model, and very similar results were observed in the metals adsorption on the green algae biomass [25].

3.5. The adsorption isotherms and adsorption capacity

The Langmuir and Freundlich isotherm models were always used to describe the participation behavior in solid-liquid systems. The Langmuir model is based on the assumption that monolayer adsorption onto a surface containing a finite number of identical sites, the active energy of adsorption in the whole process is constant, and there is no transmigration of adsorbate in the plane of the surface [27]. The linear form of Langmuir isotherm equation as follows:

$$\frac{C_e}{q_e} = \frac{1}{K_L q_{\max}} + \frac{C_e}{q_{\max}} \tag{6}$$

where q_e is the equilibrium adsorption capacity, mg g^{-1}; C_e is the equilibrium concentration of sorbate, mg L^{-1}; $q_{\max}$ is the maximum adsorption capacity, mg g^{-1}; K_L is

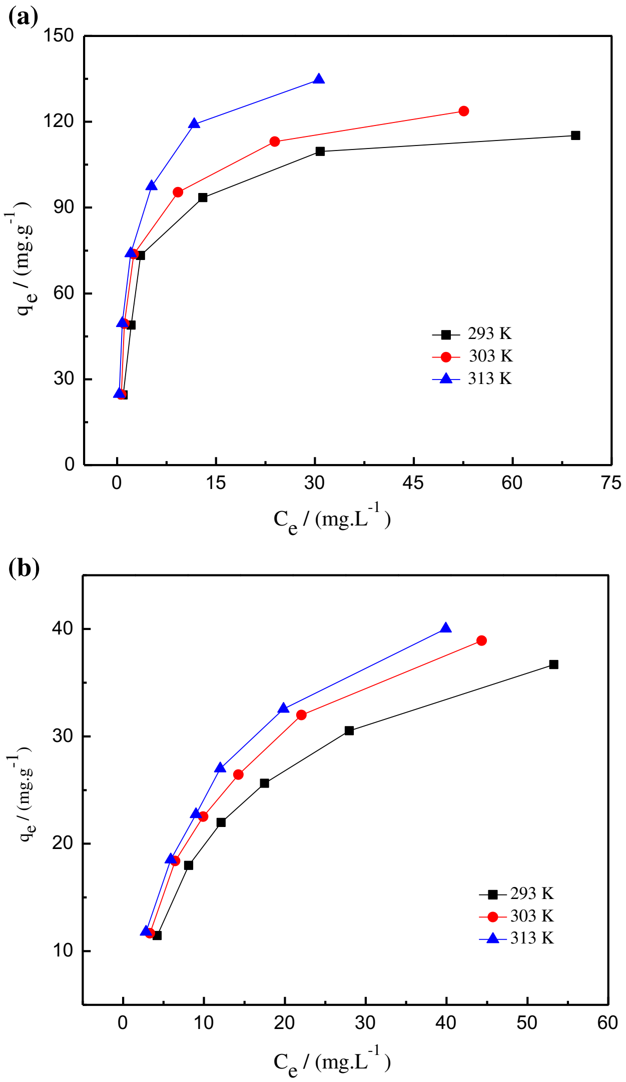

Fig. 7. Adsorption isotherms of (a) CV and (b) Pb(II) on CA-COS at different temperatures.

Table 2
Calculated constants of adsorption isotherms

		Langmuir model			Freundlich model		
Sorbate	Temperature (K)	$q_{\max}$ (mg g^{-1})	K_L (L mg^{-1})	R^2	K_F	n	R^2
CV	293	120.482	0.3138	0.9996	44.1037	4.0549	0.8724
	303	128.535	0.4023	0.9990	49.2156	4.0127	0.9043
	313	141.844	0.5357	0.9990	55.6067	3.5868	0.9377
Pb(II)	293	45.167	0.0783	0.9992	7.7940	2.5097	0.9727
	303	48.239	0.0912	0.9988	8.5978	2.4534	0.9750
	313	49.652	0.1004	0.9982	9.1055	2.4332	0.9767

Langmuir constant, L mg^{-1}. The value of K_L and $q_{\max}$ were calculated from the intercept and slope of the linear plots of C_e/q_e vs. C_e, respectively.

The Freundlich isotherm is used to describe the high concentration of adsorbate and heterogeneous surface adsorption behavior, which is not restricted to the formation of the monolayer of adsorbate. The Freundlich isotherm equation is expressed as:

$$q_e = K_F \times C_e^{\frac{1}{n}} \tag{7}$$

where q_e is the equilibrium adsorption capacity, mg g^{-1}; C_e is the equilibrium concentration of sorbate, mg L^{-1}; K_F is Freundlich constant; n is a constant which represents the degree of dependence of adsorption on the equilibrium concentration of adsorbates.

The adsorption isotherms of CV and Pb(II) at different temperatures were shown in Fig. 7, and the models mentioned above were used to fit the adsorption data, and the calculated parameters were listed in Table 2. It can be seen from the results that the experimental data fitted the Langmuir model much better than that of Freundlich model; the correlation coefficients (R^2) were all higher than 0.998, indicating the applicability of the monolayer adsorption assumption for CV and Pb(II) on CA-COS. The adsorption temperature has obvious influence in the adsorption behavior, with the temperature increased from 20 to 40˚C, the maximum adsorption capacity ($q_{\max}$) of CV and Pb(II) increased from 120.48 to 141.84 mg g^{-1} and

Table 3
The maximum adsorption of CV and Pb(II) on various adsorbents in literature

Sorbate	Adsorbent	Maximum sorption capacity (mg g^{-1})	Refs.
CV	Grapefruit peel	254.16	[8]
	CA-COS	120.48	This study
	Ricinus communis pericarp carbon	106.95	[28]
	Tomato plant root	94.33	[29]
	Skin almonds waste	85.47	[30]
	Ananas comosus leaf powder	78.22	[15]
	Ginger waste	64.93	[31]
	NaOH-modified rice husk	44.87	[9]
	Coniferous pinus bark powder	32.78	[10]
	Calotropis procera leaf	4.14	[32]
Pb(II)	*Durvillaea antarctica*	135.10	[33]
	Cucumis melo	75.42	[34]
	Moss plant *barbula lambarenensis*	62.50	[35]
	Olive tree pruning waste	46.21	[36]
	CA-COS	45.17	This study
	Hazelnut shell	28.18	[37]
	Barley straw	23.21	[38]
	Chestnut shell	8.53	[12]
	Almond shell	8.08	[37]
	Betel-nut peel	2.02	[39]

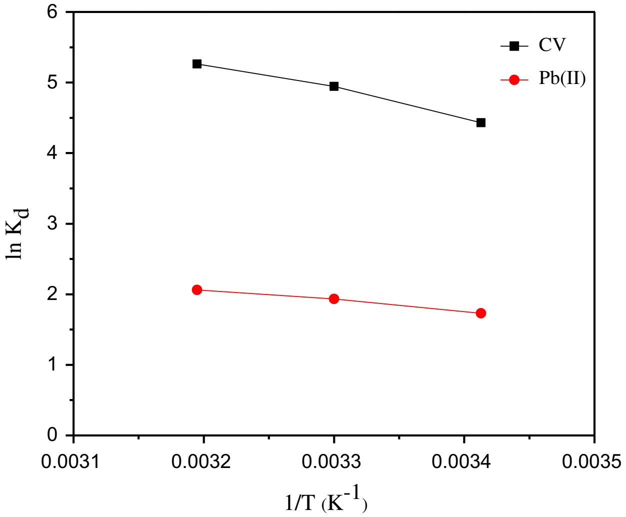

Fig. 8. Plot of ln K_d vs. $1/T$ for the estimation of thermodynamic parameters.

Table 4
Thermodynamic parameters for the adsorption of CV and Pb(II) onto CA-COS

	CV			Pb(II)		
T/K	293	303	313	293	303	313
ΔG° (kJ mol^{-1})	−10.794	−12.459	−13.696	−4.218	−4.869	−5.361
ΔH° (kJ mol^{-1})	31.796			12.554		
ΔS° (J mol^{-1} K^{-1})	145.582			57.325		

45.18 to 49.65 mg g^{-1}, respectively. The results showed that CV and Pb(II) adsorption in CA-COS may be endothermic process, higher temperature has an optimistic effect on the adsorption. Table 3 summarizes the $q_{\max}$ of various bioadsorbents on adsorption of CV and Pb(II) reported in other studies. The results showed that the adsorption capacity of the CA-COS is very comparable with those low-cost biosorbents. Some biosorbents such as grape peel or Durvillaea antarctica presented much favorable adsorption capacity to the contaminants, but compared with the COS studied in our work, the sources of the materials may be a little limited.

3.6. Thermodynamic parameters

The thermodynamic parameters that of ΔH° and ΔS° were obtained which based on the above thermodynamic experiments from the van't Hoff equation:

$$\ln K_\mathrm{d} = \frac{\Delta S^\circ}{R} - \frac{\Delta H^\circ}{RT} \tag{8}$$

where R is gas constant, 8.314 J mol^{-1} K^{-1}; T is absolute temperature, K; and K_d is thermodynamic equilibrium constant. ΔH° is the standard entropy, J mol^{-1} K^{-1}, and ΔS° is the standard enthalpy, J mol^{-1}. The ΔH° and ΔS° values were calculated from the slope and intercept of the linear plot of $\ln K_\mathrm{d}$ vs. $1/T$ (Fig. 8). The thermodynamic parameters for CV and Pb(II) adsorption on CA-COS were listed in Table 4.

The standard Gibbs free energy (ΔG°, kJ mol^{-1}) was calculated from the Gibbs–Helmholtz equation:

$$\Delta G^\circ = -RT \ln K_\mathrm{d} \tag{9}$$

The ΔG° values of CV and Pb(II) adsorbed on CA-COS under different temperatures are also presented in Table 4. It can be seen that the ΔG° values were all negative, and the higher of the temperature, the smaller of the ΔG° values obtained, which indicating that the adsorption of CV and Pb(II) on CA-COS was spontaneous process. The positive value of the standard entropy was 34.880 and 12.554 kJ mol^{-1} for CV and Pb(II), respectively, which showed that the endothermic nature of the overall adsorption process.

4. Conclusions

An adsorbent material of CA-COS was obtained by modifying the raw COS using CA via esterification. The CA-COS showed high adsorption capacity toward CV and Pb(II), and the adsorption data fitted the Langmuir model very well ($R^2 \geq 0.998$). At 293 K, the adsorption capacity of CV and Pb(II) onto CA-COS was 120.48 and 45.17 mg g^{-1} at, respectively. The adsorption process of CV and Pb(II) onto CA-COS followed the pseudo-second-order kinetic model, suggesting that the chemical interactions which occurred between superficial functional groups of biosorbent and the contaminants may be primary interaction that influence their adsorption on CA-COS. For CV, intraparticle diffusion and surface diffusion also play very important role in the adsorption. The thermodynamic results showed that adsorption was spontaneous and endothermic process.

Acknowledgments

This work was supported by the National Natural Science Foundation of China (No. 21165013, 21366024 and 21205058) and the Jiangxi Province Science Foundation for Youths (No. 20114BAB213016).

References

[1] G. Annadurai, R.S. Juang, D.J. Lee, Use of cellulose-based wastes for adsorption of dyes from aqueous solutions, J. Hazard. Mater. 92 (2002) 263–274.

[2] M. Eloussaief, M. Benzina, Efficiency of natural and acid-activated clays in the removal of Pb(II) from aqueous solutions, J. Hazard. Mater. 178 (2010) 753–757.

[3] E. Keleş, A.K. Özer, S. Yörük, Removal of Pb^{2+} from aqueous solutions by rock phosphate (low-grade), Desalination 253 (2010) 124–128.

[4] M.S. Sajab, C.H. Chia, S. Zakaria, S.M. Jani, M.K. Ayob, K.L. Chee, P.S. Khiew, W.S. Chiu, Citric acid modified kenaf core fibres for removal of methylene blue from aqueous solution, Bioresour. Technol. 102 (2011) 7237–7243.

[5] G.O. El-Sayed, Removal of methylene blue and crystal violet from aqueous solutions by palm kernel fiber, Desalination 272 (2011) 225–232.

[6] R. Gong, S. Zhu, D. Zhang, J. Chen, S. Ni, R. Guan, Adsorption behavior of cationic dyes on citric acid esterifying wheat straw: Kinetic and thermodynamic profile, Desalination 230 (2008) 220–228.

[7] B. Opeolu, Utilization of maize (*Zea mays*) cob as an adsorbent for lead(II) removal from aqueous solutions and industrial effluents, Afr. J. Biotechnol. 8 (2009) 1567–1573.

[8] A. Saeed, M. Sharif, M. Iqbal, Application potential of grapefruit peel as dye sorbent: Kinetics, equilibrium and mechanism of crystal violet adsorption, J. Hazard. Mater. 179 (2010) 564–572.

[9] S. Chakraborty, S. Chowdhury, P. Das Saha, Adsorption of Crystal Violet from aqueous solution onto NaOH-modified rice husk, Carbohydr. Polym. 86 (2011) 1533–1541.

[10] R. Ahmad, Studies on adsorption of crystal violet dye from aqueous solution onto coniferous pinus bark powder (CPBP), J. Hazard. Mater. 171 (2009) 767–773.

[11] J. X. Yu, L.Y. Wang, R.A. Chi, Y.F. Zhang, Z.G. Xu, J. Guo, Competitive adsorption of Pb^{2+} and Cd^{2+} on magnetic modified sugarcane bagasse prepared by two simple steps, Appl. Surf. Sci. 268 (2013) 163–170.

[12] G. Vázquez, M. Calvo, M. Sonia Freire, J. González-Alvarez, G. Antorrena, Chestnut shell as heavy metal adsorbent: Optimization study of lead, copper and zinc cations removal, J. Hazard. Mater. 172 (2009) 1402–1414.

[13] K. Xue, L. Yan, W. Lai, Z. Huang, H. Guo, Ultrasonic-microwave-enzyme synergistic extraction of proanthocyanidins from *Camellia oleifera* shell, Chem. Res. Appl. 24 (2012) 1295–1299.

[14] D. Song, H. Guo, L. Yan, Study on adsorptive property of crystal violet on *cemellia oleifera* shell in aqueous solution, Chin. J. Environ. Eng. 8 (2014) 214–219.

[15] S. Chakraborty, S. Chowdhury, P.D. Saha, Insight into biosorption equilibrium, kinetics and thermodynamics of crystal violet onto *Ananas comosus* (pineapple) leaf powder, Appl. Water Sci. 2(2) (2012) 135–141.

[16] R. Gong, Y. Jin, F. Chen, J. Chen, Z. Liu, Enhanced malachite green removal from aqueous solution by citric acid modified rice straw, J. Hazard. Mater. 137 (2006) 865–870.

[17] G. Tan, H. Yuan, Y. Liu, D. Xiao, Removal of lead from aqueous solution with native and chemically modified corncobs, J. Hazard. Mater. 174 (2010) 740–745.

[18] N. Feng, X. Guo, Characterization of adsorptive capacity and mechanisms on adsorption of copper, lead and zinc by modified orange peel, Trans. Nonferrous Met. Soc. China 22 (2012) 1224–1231.

[19] J. Zhu, P. Wang, X.F. Wu, W. Luo, M. Lei, Adsorption of Pb^{2+} ions on diatomite modified by polypropylene acetamide and bariumchloride in aqueous solution, Afr. J. Agric. Res. 7 (2012) 3614–3620.

[20] A. Hashem, E. Abdel-Halim, K.F. El-Tahlawy, A. Hebeish, Enhancement of the adsorption of Co(II) and Ni(II) ions onto peanut hulls through esterification using citric acid, Adsorpt. Sci. Technol. 23 (2005) 367–380.

[21] B. Zhu, T. Fan, D. Zhang, Adsorption of copper ions from aqueous solution by citric acid modified soybean straw, J. Hazard. Mater. 153 (2008) 300–308.

[22] S. Ibrahim, M. Megat Hanafiah, F. Fadzil, F. Fadzil, Adsorption of lead ions onto citric acid modified rubber (*Hevea brasiliansis*) leaves, Adv. Mater. Res. 896 (2014) 288–291.

[23] T. Vaughan, C.W. Seo, W.E. Marshall, Removal of selected metal ions from aqueous solution using modified corncobs, Bioresour. Technol. 78 (2001) 133–139.

[24] V.K. Gupta, R. Jain, S. Varshney, Removal of Reactofix golden yellow 3 RFN from aqueous solution using wheat husk—An agricultural waste, J. Hazard. Mater. 142 (2007) 443–448.

[25] D. Bulgariu, L. Bulgariu, Equilibrium and kinetics studies of heavy metal ions biosorption on green algae waste biomass, Bioresour. Technol. 103 (2012) 489–493.

[26] J. Bujdák, P. Komadel, Interaction of methylene blue with reduced charge montmorillonite, J. Phys. Chem. B 101 (1997) 9065–9068.

[27] X. Li, W. Zheng, D. Wang, Q. Yang, J. Cao, X. Yue, T. Shen, G. Zeng, Removal of Pb(II) from aqueous solutions by adsorption onto modified areca waste: Kinetic and thermodynamic studies, Desalination 258 (2010) 148–153.

[28] S. Madhavakrishnan, K. Manickavasagam, R. Vasanthakumar, K. Rasappan, R. Mohanraj, S. Pattabhi, Adsorption of crystal violet dye from aqueous solution using *Ricinus communis* pericarp carbon as an adsorbent, J. Chem. 6 (2009) 1109–1116.

[29] C. Kannan, N. Buvaneswari, T. Palvannan, Removal of plant poisoning dyes by adsorption on Tomato Plant Root and green carbon from aqueous solution and its recovery, Desalination 249 (2009) 1132–1138.

[30] F. Atmani, A. Bensmaili, N. Mezenner, Synthetic textile effluent removal by skin almonds waste, J. Environ. Sci. Technol. 2 (2009) 153–169.

[31] R. Kumar, R. Ahmad, Biosorption of hazardous crystal violet dye from aqueous solution onto treated ginger waste (TGW), Desalination 265 (2011) 112–118.

[32] H. Ali, S.K. Muhammad, Biosorption of crystal violet from water on leaf biomass of *Calotropis procera*, J. Environ. Sci. Technol. 1 (2008) 143–150.

[33] H.K. Hansen, C. Gutierrez, J. Callejas, C. Cameselle, Biosorption of lead from acidic aqueous solutions using *Durvillaea antarctica* as adsorbent, Miner. Eng. 46–47 (2013) 95–99.

[34] S. Tunali Akar, S. Arslan, T. Alp, D. Arslan, T. Akar, Biosorption potential of the waste biomaterial obtained from *Cucumis melo* for the removal of Pb^{2+} ions from aqueous media: Equilibrium, kinetic, thermodynamic and mechanism analysis, Chem. Eng. J. 185–186 (2012) 82–90.

[35] B.I. Olu-Owolabi, P.N. Diagboya, W.C. Ebaddan, Mechanism of Pb^{2+} removal from aqueous solution using a nonliving moss biomass, Chem. Eng. J. 195–196 (2012) 270–275.

[36] O. Uzunosmanoglu, A. Uyanik, M.S. Engin, The removal of cadmium(II), copper(II) and lead(II) from aqueous solutions by olive tree pruning waste, Fres. Environ. Bull. 20 (2011) 3135–3140.

[37] E. Pehlivan, T. Altun, S. Cetin, Iqbal Bhanger M., Lead sorption by waste biomass of hazelnut and almond shell, J. Hazard. Mater. 167 (2009) 1203–1208

[38] E. Pehlivan, T. Altun, S. Parlayıcı, Utilization of barley straws as biosorbents for Cu^{2+} and Pb^{2+} ions, J. Hazard. Mater. 164 (2009) 982–986.

[39] M.A. Rahman, M.A. Hasan, M.A. Salam, A. Salam, Betel-nut peel as an adsorbent in the removal of Cd, Cr and Pb from aqueous solutions, Pak. J. Anal. Environ. Chem. 13 (2012) 137–147.